Enhancing Image for CNN-based Diagnostic of Pediatric Pneumonia through Chest Radiographs

Vaishali Arya, Tapas Kumar

Department of CSE, FET, Manav Rachna International Institute of Research and Studies, Faridabad, India

Abstract—In underdeveloped nations, severe lower respiratory infections are the principal reasons of infant mortality. The best treatments and early diagnosis are now being used to alleviate this issue. In developing nations, better treatment and prevention approaches are still required. Clinical, microbial, and radiographic clinical studies have a broad range of applicability within and across populations, and it much depends on the knowledge and resources that are made accessible in different situations. The most appropriate procedure is a chest radiograph (CXR), although pediatric chest X-ray techniques using machine intelligence are uncommon. A strong system is required to diagnose pediatric pneumonia. Authors provide a computer-aided diagnosis plan for the chest X-ray scans to address this. This investigation provides a deep learning-based intelligent healthcare that can reliably diagnose pediatric pneumonia. In order to improve the appearance of CXR pictures, the suggested technique also employs white balancing accompanied with contrast enhancement as a preliminary step. With an AUC of 99.1 on the testing dataset, the suggested approach outscored other state-of-the-art approaches and produced impressive results. Additionally, the suggested approach correctly classified chest X-ray scans as normal and pediatric pneumonia with a classification accuracy of 98.4%.

Keywords—Contrast enhancement; convolution neural network; pediatric pneumonia; radiography; white balancing

I. INTRODUCTION

The most prevalent pathogens being the reason of mortality in kids is pneumonia. Pneumonia is a disease caused by infections such as viruses, bacteria, and fungi that enter the lungs and cause the alveoli to fill with inflammatory fluid. It's crucial to get this condition diagnosed early since it has devastating consequences, particularly in kids under the age of five, and can be controlled by doing so. More than 150 million kids below the age of five are affected with pneumonia annually, and 20 million of kids require hospitalization for treatment [1]. The most of pneumonia infections occur in developing and underdeveloped countries, where there is a lack of medical services, excessive urbanisation, pollution, and unclean air. Therefore, avoiding the condition from turning deadly can be greatly aided by early treatment and detection.

The conventional biological diagnostics are inadequate to determine the cause of pediatric pneumonia since blood cultures are insensitive, pulmonary aspirates are difficult to collect, and antigen assays have poor specificity [2]. Presently, the diagnosis of pneumonia is determined by the patient's symptoms, the results of a CXR, the growth and susceptibility of the bacteria found in throat swabs or sputum specimens, and blood tests. Early detection of pediatric pneumonia is crucial in reducing repercussions since this illness is curable and may be prevented, particularly through vaccines. CXRs, while having a lower resolution than Magnetic Resonance Imaging (MRI) or Computerized Tomography (CT) scans, can nevertheless be utilized to conduct a wide range of evaluations. Radiographic diagnosis of pediatric pneumonia is very subjective and is reliant on the radiologist's skill and understanding. High definition MRI and CT scans make it simpler to detect pneumonia, though most radiologists prefer to utilize CXRs for evaluations due to the faster turnaround time and economical nature of the technology. Radio-opacities or white patches in the airways, especially in the alveoli, are typically seen on a scan of pneumonia and signify the existence of chronic effusion. Attributed to the reason that some illnesses might resemble similar indications, these radiological observations can be challenging for a trainee radiologist and result in incorrect positives and negatives. Fig. 1 displays examples of CXR pictures from the pediatric population that have been categorized as normal and pneumonia for this research.

Artificial intelligence (AI) has notably been utilized to diagnose pneumonia-related abnormalities in radiographic scans. Deep Learning (DL) techniques are the most well-known and commonly used approach for detecting and classifying clinical pictures in general, and pneumonia specifically, owing to the abundance of tagged CXR resources and ubiquitous, reasonably priced computer capacity. These technologies carry the potential and can diagnose numerous illnesses with conventional physician precision [3].

In earlier investigations, various unique data pre-processing methods have been demonstrated to be helpful in a wide range of applications [4], including voice recognition, hand motion detection utilizing sonography [5], and hand motion identification utilising navigation systems [6]. In the job of classifying natural photographs, Convolutional Neural Networks (CNNs) has demonstrated excellent outcomes. Clinical scans, on the other hand, can be found in three-dimensional RGB, four-dimensional, or two-dimensional with grayscale files, whilst natural photographs are often found in two dimensional RGB file types. This necessitates a lot of adjusting. Another important distinction relates to illumination changes. In addition, natural images are typically recognised by their edges, fundamental shapes, relationships between nearby pixels, etc., while each pixel's illuminance extent or severity are not important characteristics for their identification. Conversely, when it comes to clinical scans, particularly CXR scans, each pixel's luminance is key for identifying the image's impacted areas. This is incredibly important for spotting anomalies in CXR scans. So, developing

a reliable and effective model for spotting anomalies in clinical scans requires good image pre-processing. Thus, current study adopts a technique that combines white balance and contrast enhancement as a stage in the pre-processing of input for picture improvement.
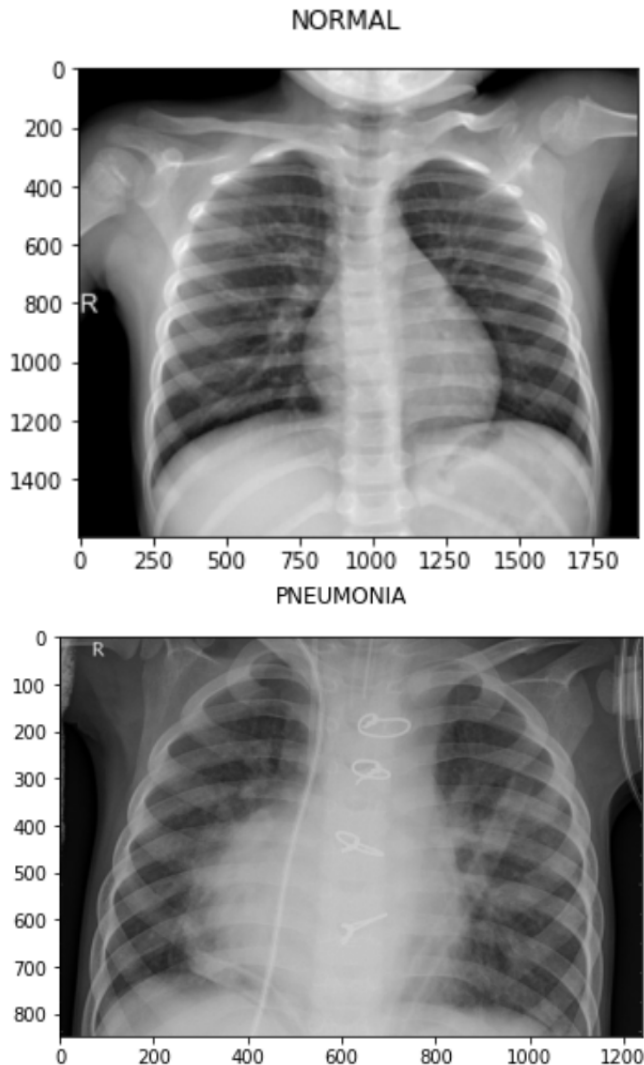
NORMAL

PNEUMONIA

Fig. 1. Samples of CXR images.

The system takes advantage of a multi-layered CNN to accurately predict pneumonia by automatically extracting information from radiography scans. While screening pediatric pneumonia, computer assisted diagnostic (CAD) technologies can take the place of radiologist discretion. They are also useful in rural places or nations without access to technology, such as radiological competence, to corroborate diagnostic evidence. This study suggests a cutting-edge model that can distinguish between pneumonia and the usual. The key contributions of this research are listed below.

- With a remarkable good accuracy of 98.4%, the new proposed design can differentiate between pediatric pneumonia and normal.

- In addition to accuracy, the model's sensitivity, specificity, precision, and F1-score are all 0.9841, 0.9837, 0.9898, and 0.9867, respectively.

- The error symbolized by the False Positives (FP) and False Negatives (FN) is close to 1.6%.

- The efficiency of the suggested design is significantly better than the most recent models stated in the literature.

The manuscript is further divided into sections. Section II highlights the related work. Section III introduces the proposed model. Section IV elaborates the experiment conducted and results achieved. Section V, finally concludes this research.

II.   RELATED WORKS

Major innovations in deep learning have made it possible to automate CXR interpretation with accuracy on par with that of professional specialists [7, 8, 9, 10]. By decreasing ambiguities in explanation and encouraging increasingly broad use of radiological outcomes in scientific studies, automating the diagnosis through CXR may increase sample performance.

Transfer learning was used by Kermany et al. [11] to build a CNN model that could identify pneumonia in CXR scans. CXR images have been classified by Rajaraman et al. [12] as diagnose bacterial and viral pneumonia using a CNN-based approach. Rather than employing the entire picture, they trained CNN models using regions of concern that only contain the lungs. A 121-layer CNN model called CheXNet was created by Rajpurkar et al. [13]. One million CXR scans with 14 distinct illnesses were used to train CheXNet. 420 CXR scans have been used to evaluate the suggested model, and the findings were contrasted to those of professional radiologists. As a consequence, it has been discovered that the CNN model outperformed radiologists generally in spotting pneumonia. A CNN model was presented by Stephen et al. [14]. They built the CNN model from the beginning to classify images from a particular CXR scan to obtain outstanding generalization ability that they utilised to assess whether or not a patient has been afflicted with pneumonia. This differs from prior methods relying simply on transfer learning or classic handmade approaches.

Liang et al. [15] used backpropagation and expanded convolution techniques to achieve pneumonia diagnosis with a CNN framework. While categorising CXR scans, they additionally identified the transfer learning impact on convolutional networks. A sequential CNN model comprising eighteen layers that automatically diagnoses pneumonia has been suggested by Siddiqi [16]. Gu et al. [17] suggested a two-stage technique for discriminating between distinct types of pneumonia. The transfer learning approach has been employed by Rahman et al. [18] to conduct the pneumonia prediction leveraging four pre-trained CNN models. They used three distinct categorization techniques to label CXR scans. Three well-known CNN models have been employed by Togacar et al. [19] for the feature extraction step. Researchers built every model independently employing the same input, and based on the final fully linked layers of every CNN, they extracted 1000 characteristics. For the pneumonia identification challenge,

1000 characteristics have been produced, and these characteristics have been used as inputs to machine learning classifier. A CapsNet CNN architecture with multi-layered containers has been introduced by Mittal et al. [20] for the detection of pneumonia in CXR scans.

III. PROPOSED MODEL

The objective of current research is to devise an automatic pediatric pneumonia recognition system that can assist in the absence of radiologist. Fig. 2 shows the strategy suggested in this research for identifying pediatric pneumonia utilizing CXR scans. The whole architecture is divided into four phases, i.e., pre-processing model, pre-trained model, interim model and outcome model.

A. Pre-processing Model

The image pre-processing model enrich the input by performing four operations i.e., image enhancement, normalization, resizing and data augmentation.

1) Image enhancement: Image enhancement start with white balancing followed by contrast enhancement. The image processing technique known as white balance is used to correct the colour integrity of a CXR scan. The scan recording technology does not perfectly capture light like the naked eye does because of the low illumination circumstances in clinical scans, which made certain portions of the scan look dark. The finished scan should thus accurately reflect the colours of the actual picture through image processing or restoration. This investigation's goal is to make the scan more visible so that the suggested model may identify important information from it. Through the separate stretching of the RGB channels, the white balance technique modifies the colours of the scan's layered structure. Stretching is done for the leftover colour range whilst discarding the pixel colours that are near the terminus of the RGB channels and are only employed by

0.05% of the pixels that comprise the scan. After this procedure, the minimum and maximum limit readings would not be adversely affected by pixel colours that were seldom existent at the channel's terminus when stretching [21]. In this solution, we have implemented a white balance as depicted in Eq. (1) and Eq. (2).

$$I_p = \frac{1}{3}\left(\sum_{i \in R,G,B} \frac{1}{W*H} \sum_{x=1}^{W} \sum_{y=1}^{H} \text{image}_i(x,y)\right) * p\% \quad (1)$$

$$\text{Image}_{\text{white\_balance}} = \text{Sat}\left(\frac{\sum_{i \in R,G,B} \text{image}_i - I_p * 255}{I_{99.05} - I_{0.05}}\right) \quad (2)$$

where I_p denotes the pth aggregate percent of RGB channels, and Sat() performs saturation operation within the range of (0,255). $\text{Image}_{\text{white\_balance}}$ presents the white balanced channels pixel values.

After the white balancing, contrast enhancement is achieved through Contrast Limited Adaptive Histogram Equalization (CLAHE) [22], which is an upgradation of adaptive histogram equation (AHE) [23]. AHE divides the original picture into a number of smaller pictures, sometimes referred to as tiles. This approach employs the intensity rebinding algorithm for every tile to be derived from the histogram of every tile, which is generated and correlates to various regions of the picture.

This technique over-intensifies the image, which brings noise into the picture [23]. To handle this noise, authors adopt the CLAHE algorithm. The CLAHE algorithm operates exactly like the AHE algorithm, except before generating the continuous distribution function, it slices the histogram at particular values to restrict the intensification. The histogram's over-intensified portion is further dispersed throughout the histogram. CLAHE had remarkable results in improving CXR scans in one of the earlier research [24] and was deemed helpful in analysing a wide range of medical pictures.
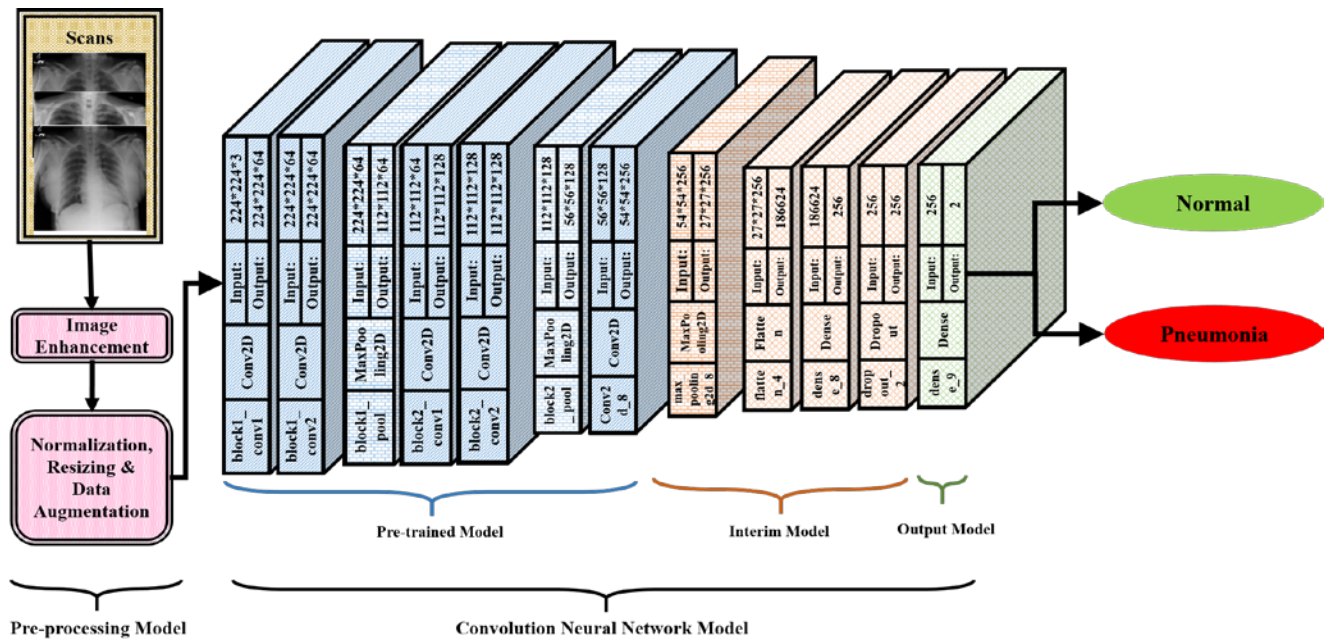

Fig. 2. Proposed model.

2) Normalization, resizing & data augmentation: Low-quality or low-resolution CXR scans have not been excluded; all of the CXR scans have been used, normalised, and resized to 224*224*3 as the current proposal specifies. A huge collection is needed for the neural network to be trained effectively. CNN models rarely generalise when built on a smaller dataset, which results in low test performance [25, 26]. One approach to resolving this issue is data augmentation, which effectively enhances the underlying dataset. There have been 3883 pneumonia-infected CXR scans and 1349 normal CXR scans in the train set employed in this research. Just the scans of the normal case have been augmented two times since the collection already provided adequate scans of the pneumonia incident. Authors augmented the CXR scans in three steps considering that not all augmentation techniques worked well with CXR images: *i)* random flipping (to negotiate directly with pneumonia signs on every edge of the CXR), *ii)* random shearing (to get a profound understanding of the relationship between pixels), and, *iii)* differing rotation [27]. After augmentation, there have been 3883 scans of pneumonia and 4047 scans of normal. Scans from the testing dataset have not been enhanced.

B. Convolution Neural Network Model

The proposed CNN model is divided into three phases 1) Pre-trained model, 2) Interim model, and 3) Outcome model.

1) Pre-trained model: The pre-processed scans are stuffed as input to the pre-trained model. This phase of the proposed model is a CNN framework with two convolution filtering layers on top and one pooling layer. Subsequently, one pooling layer and three convolution filtering layers are applied twice. The SoftMax conclusion is the result of three entirely interconnected layers that make up the architecture's intellect. One million ImageNet [7] annotated images with 224*224*3 colour images assigned to 1000 class labels are used to pre-train the classifiers. Authors have chosen the top seven layers of this framework to serve as our pre-trained model.

2) Interim model: Given the fact that our intended collection of CXR scans comprises "big 3-channeled images," authors initially make minor restructuring to the pre-trained model while keeping its core values. Through our own unique layers, we deliberately altered the final grades of the initial model. Our method employs three filters to create a three-channel extracted features while maintaining kernel size and latency hyper-parameters that are similar to the primary convolutional of the original incarnation. Authors utilize the legitimate activation function while applying the preliminary idea. Authors want to refine the previous concept for a "middleman" zone while both training and developing the layers to get the interim model. The last level of the interim phase is modified to anticipate certain classes since the large clinical images are more akin to CXR scans. This model's outcome is identical to the preceding tightly compacted layer input, with arbitrary vertices set to zero. The result would be labeled as $Output_{interim}$.

3) Outcome model: In order to connect the interim model results to the arena of CXR scan, which constitutes a last dense layer employing "softmax" activation function, authors adopt 224*224*3 inputs obtained from pre-trained model. Researchers can use a larger input dimension in addition to the advantage of translating a model of imaging modalities to the CXR arena. This has the benefit of producing more distinctive patterns since larger pictures contain greater info. Authors include a pre-trained model using the 3-channeled images from the result zone after 50 epochs of the interim solution. This output model distinguishes between normal and pediatric as $Output_{final}$.

$$Output_{final} = max\_index \left(\frac{e^{Output_{interim\_i}}}{e^{i1} + e^{i2}} \right) \qquad (3)$$

where, $Output_{interim\_i}$ denotes the input vector, e^i presents the exponential function and max_index() operation calculates the index of class (i.e., 1 or 2) depicted by maximum instances of input vector.

IV. EXPERIMENTS AND RESULTS

This section provides the precise details of the tests that have been carried out to evaluate the suggested framework. The CNN model have been implemented using the Keras toolkit alongside TensorFlow. On a machine featuring 64 GB of RAM and an NVIDIA 1080 Ti graphics card, processing has been conducted.

A. Dataset

CXR scans of kids are much more troublesome than those of grownups. Particularly, poor posture and even the existence of limbs like arms and necks pose a challenge to educate the network and locate the pneumonia that is associated with the issue. A collection of CXR scans collected by Kermany et al. [28] has been employed in the investigation. This dataset comprises of 5856 scans of kids between the ages of one and five that have been classified as pneumonia and normal by qualified radiologists. Two subgroups of the training examples in the dataset have been provided: 1349 normal scans and 3883 pneumonia scans. Similarly, the testing dataset in the scans have been split into 234 normal scans and 390 pneumonia scans. 20% of the training examples has been employed for validation, and the remaining 80% for training. The adopted dataset has already secured the testing data. This data collection has been employed in several academic investigations, and various categorization techniques have been applied on it [29].

B. Results

The proposed framework has been trained to distinguish between scans of pediatric pneumonia and scans of normal CXR, and the prototype appears to have learnt how to address this issue successfully and effectively. It appears to have been successful in locating the properties associated with the particular category. Fig. 3 and Fig. 4 depict the accuracy and loss attained in the proposed model corresponding to 50 epochs, respectively. Considering accuracy and loss values, the suggested model generated the highest outcomes.
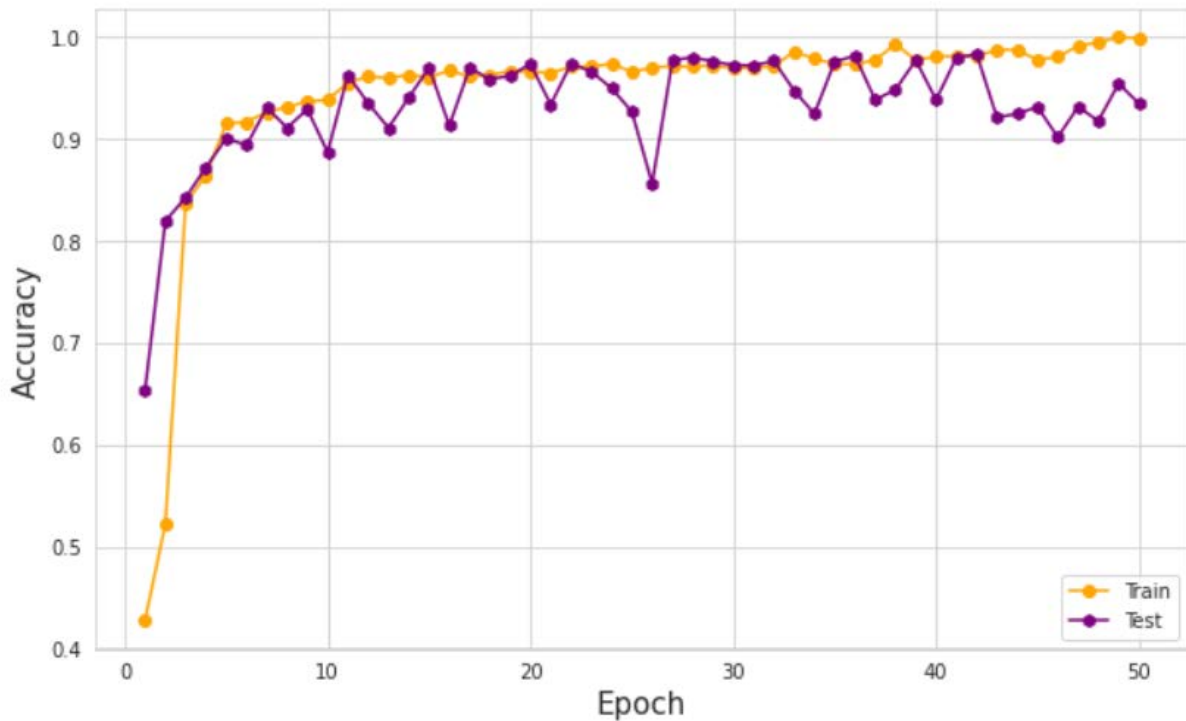
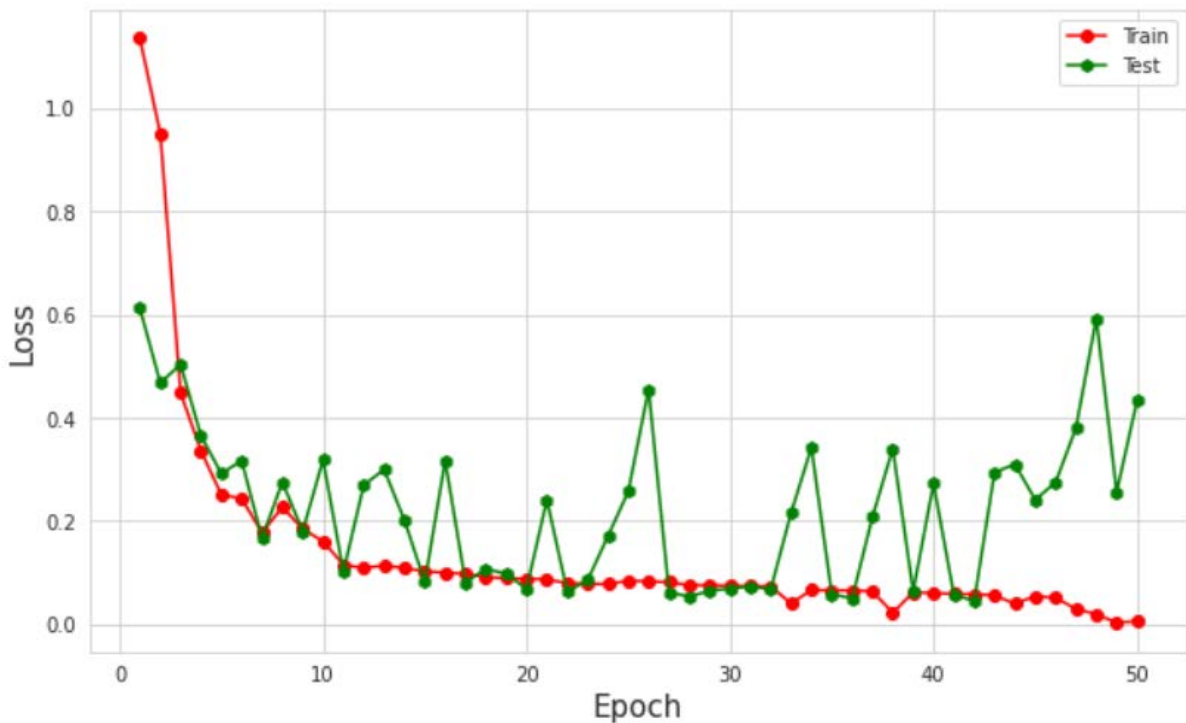Fig. 3.   Accuracy comparison of training and testing dataset.

Fig. 4.   Loss comparison of training and testing dataset.

The confusion matrix is depicted graphically in Fig. 5 of the classifier's effectiveness, in which the rows correspond to the forecasts and the columns to the original category. The amount of correctly and incorrectly classified scans is shown in the confusion matrix, and it is evident that the suggested framework has been able to distinguish between the underlying categories with 98.4% accuracy. Further, the error symbolized by the False Positives (FP) and False Negatives (FN) is close to 1.6%. In addition to accuracy, the model's sensitivity, specificity, precision, and F1-score are all 0.9841, 0.9837, 0.9898, and 0.9867, respectively.

Fig. 5.   Confusion matrix.

The Receiver Operating Characteristic (ROC) curve for the suggested model is depicted in Fig. 6. The curve illustrates is a critical performance indicator for every classification model. The AUC is approximately one (0.991 for pneumonia and 0.986 for normal) and the slope in the graph is extremely close to the upper left corner, showing excellent result in differentiating between the two categories. The curve also demonstrates that the suggested model's capacity to distinguish between pediatric pneumonia and normal is nearly comparable.
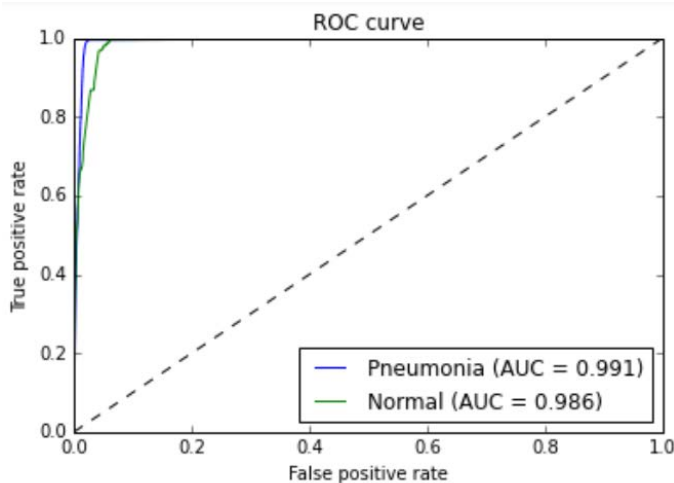

Fig. 6.   Receiver operating characteristic curve.

C. Comparative Study with State-of-the-Art Methods

In Table I, a comparison research is shown. The suggested approach is compared against other prevailing techniques' accuracy. In order to classify cases of pneumonia, Liang et al. [15], Zubair et al. [30], and Mahmud et al. [31] employed simple transfer learning techniques and reached accuracy levels of 90.5%, 96.6%, and 98.1%, respectively. Using specially designed CNNs, Rajaraman et al. [12] have been able to attain an accuracy of 96.2%. An accuracy of 96.36% has been obtained by Chouhan et al. [32] who developed an ensemble model to aggregate estimates from various deep learning

algorithms. The quantity of deep features has been decreased by Togacar et al. [19], who claimed accuracy of 96.84%. An accuracy of 98.0% was attained by Rahman et al. [18] using CNNs. Hashmi et al. [33] attained an accuracy of 98.3%. The strategy proposed in current research performed better than the existing approaches and achieved an accuracy of 98.4% with precision, recall, and AUC of 0.9898, 0.9841, and 0.991, respectively.

TABLE I.   COMPARISON WITH STATE-OF-THE-ART METHODS

Model	Accuracy	Precision	Recall	AUC
Liang et al. [15]	90.50%	0.891	0.967	0.927
Rajaraman et al. [12]	96.20%	0.962	0.995	0.993
Chouhan et al. [32]	96.39%	0.9328	0.996	0.9934
Zubair et al. [30]	96.60%	0.972	0.981	-
Togacar et al. [19]	96.84%	0.9688	0.9683	0.968
Rahman et al. [18]	98.00%	0.97	0.99	0.98
Mahmud et al. [31]	98.10%	0.98	0.985	0.983
Hashmi et al. [33]	98.30%	0.9825	0.9814	0.9971
Proposed Model	98.40%	0.9898	0.9841	0.991

V.   CONCLUSIONS

The most common cause of mortality for kids under the age of five globally is pneumonia. Chest X-rays are evaluated by qualified radiologists to diagnose pneumonia. However, it takes a lot of time and is tiresome. Methodologies for biomedical image diagnostics have a lot of potential for use in clinical image analysis. In this study, authors provide an efficient deep learning algorithm for more accurate pediatric pneumonia detection from CXR scans. By using sophisticated pre-processing techniques to render CXR scans more visible, the suggested method collects low-level feature space, enabling recognition of complicated trends from clinical scans on a par with skilled radiologists. The suggested approach may aid in illness detection and support radiologists in the patient care. To evaluate the effectiveness of the suggested model, several metrics, including accuracy, sensitivity, specificity, precision, and AUC score, are calculated. On the testing dataset, the suggested model achieved a precision of 0.9898, an F1-score of 0.9867, an AUC score of 0.991, a sensitivity of 0.9841, a specificity of 0.9837, and an accuracy of 98.4%. Furthermore, based on the current evaluation criteria, the suggested model beats cutting-edge architectures.

REFERENCES

[1]   I. Rudan, C. Boschi-Pinto, Z. Biloglav, K. Mulholland and H. Campbell, "Epidemiology and etiology of childhood pneumonia," *Bulletin of the world health organization,* vol. 86, pp. 408-416B, 2008.

[2]   T. Cherian, E. K. Mulholland, J. B. Carlin, H. Ostensen, R. Amin, M. D. Campo, D. Greenberg, R. Lagos, M. Lucero, S. A. Madhi and K. L. O'Brien, "Standardized interpretation of paediatric chest radiographs for the diagnosis of pneumonia in epidemiological studies," *Bulletin of the World Health Organization,* vol. 83, pp. 353-359, 2005.

[3]   N. Liu, L. Wan, Y. Zhang, T. Zhou, H. Huo and T. Fang, "Exploiting convolutional neural networks with deeply local description for remote sensing image classification," *IEEE access,* vol. 6, pp. 11215-11228, 2018.

[4]   S. Batra, R. Khurana, M. Z. Khan, W. Boulila, A. Koubaa and P. Srivastava, "A Pragmatic Ensemble Strategy for Missing Values Imputation in Health Records," *Entropy,* vol. 24, no. 4, p. 533, 2024.

[5]   J. W. Picone, "Signal modeling techniques in speech recognition," *Proceedings of the IEEE,* vol. 81, no. 9, pp. 1215-1247, 1993.

[6]   S. Hazra and A. Santra, "Robust gesture recognition using millimetric-wave radar system," *IEEE sensors letters,* vol. 2, no. 4, pp. 1-4, 2018.

[7]   J. Deng, W. Dong, R. Socher, L. J. Li, K. Li and L. Fei-Fei, "Imagenet: A large-scale hierarchical image database," in *2009 IEEE conference on computer vision and pattern recognition*, 2009.

[8]   J. Irvin, P. Rajpurkar, M. Ko, Y. Yu, S. Ciurea-Ilcus, C. Chute, H. Marklund, B. Haghgoo, R. Ball, K. Shpanskaya and J. Seekins, "Chexpert: A large chest radiograph dataset with uncertainty labels and expert comparison," in *Proceedings of the AAAI conference on artificial intelligence*, 2019.

[9]   P. Rajpurkar, J. Irvin, R. L. Ball, K. Zhu, B. Yang, H. Mehta, T. Duan, D. Ding, A. Bagul, C. P. Langlotz and B. N. Patel, "Deep learning for chest radiograph diagnosis: A retrospective comparison of the CheXNeXt algorithm to practicing radiologists," *PLoS medicine,* vol. 15, no. 11, p. e1002686, 2018.

[10] S. Batra and S. Sachdeva, "Organizing standardized electronic healthcare records data for mining," *Health Policy and Technology,* vol. 5, no. 3, pp. 226-242, 2016.

[11] D. S. Kermany, M. Goldbaum, W. Cai, C. C. Valentim, H. Liang, S. Baxter, A. McKeown, G. Yang, X. Wu, F. Yan and J. Dong, "Identifying medical diagnoses and treatable diseases by image-based deep learning," *Cell,* vol. 172, no. 5, pp. 1122-1131, 2018.

[12] S. Rajaraman, S. Candemir, I. Kim, G. Thoma and S. Antani, "Visualization and interpretation of convolutional neural network predictions in detecting pneumonia in pediatric chest radiographs," *Applied Sciences,* vol. 8, no. 10, p. 1715, 2018.

[13] P. Rajpurkar, J. Irvin, K. Zhu, B. Yang, H. Mehta, T. Duan, D. Ding, A. Bagul, C. Langlotz, K. Shpanskaya and M. P. Lungren, "Chexnet: Radiologist-level pneumonia detection on chest x-rays with deep learning," *arXiv preprint,* 2017.

[14] O. Stephen, M. Sain, U. J. Maduh and D. U. Jeong, "An efficient deep learning approach to pneumonia classification in healthcare," *Journal of healthcare engineering,* 2019.

[15] G. Liang and L. Zheng, "A transfer learning method with deep residual network for pediatric pneumonia diagnosis," *Computer methods and programs in biomedicine,* vol. 187, p. 104964, 2020.

[16] R. Siddiqi, "Automated pneumonia diagnosis using a customized sequential convolutional neural network," in *Proceedings of the 2019 3rd international conference on deep learning technologies*, 2019.

[17] X. Gu, L. Pan, H. Liang and R. Yang, "Classification of bacterial and viral childhood pneumonia using deep learning in chest radiography," in *Proceedings of the 3rd international conference on multimedia and image processing*, 2018.

[18] T. Rahman, M. E. Chowdhury, A. Khandakar, K. R. Islam, K. Islam, Z. B. Mahbub, M. A. Kadir and S. Kashem, "Transfer learning with deep convolutional neural network (CNN) for pneumonia detection using chest X-ray," *Applied Sciences,* vol. 10, no. 9, p. 3233, 2020.

[19] M. Toğaçar, B. Ergen, Z. Cömert and F. Özyurt, "A deep feature learning model for pneumonia detection applying a combination of mRMR feature selection and machine learning models," *Irbm,* vol. 41, no. 4, pp. 212-222, 2020.

[20] A. Mittal, D. Kumar, M. Mittal, T. Saba, I. Abunadi, A. Rehman and S. Roy, "Detecting pneumonia using convolutions and dynamic capsule routing for chest X-ray images," *Sensors,* vol. 20, no. 4, p. 1068, 2020.

[21] "White Balance," [Online]. Available: https://docs.gimp.org/2.10/en/gimp-layer-white-balance.html. [Accessed 18 November 2022].

[22] A. M. Reza, "Realization of the contrast limited adaptive histogram equalization (CLAHE) for real-time image enhancement," *Journal of VLSI signal processing systems for signal, image and video technology,* vol. 38, pp. 35-44, 2004.

[23] S. M. Pizer, E. P. Amburn, J. D. Austin, R. Cromartie, A. Geselowitz, T. Greer, B. ter Haar Romeny, J. B. Zimmerman and K. Zuiderveld, "Adaptive histogram equalization and its variations," *Computer vision, graphics, and image processing,* vol. 39, no. 3, pp. 355-368, 1987.

[24] S. M. Pizer, "Contrast-limited adaptive histogram equalization: Speed and effectiveness stephen m. pizer, r. eugene johnston, james p. ericksen, bonnie c. yankaskas, keith e. muller medical image display research group," in *Proceedings of the first conference on visualization in biomedical computing*, Atlanta, Georgia, 1990.

[25] S. Batra, H. Sharma, W. Boulila, V. Arya, P. Srivastava, M. Z. Khan and M. Krichen, "An Intelligent Sensor Based Decision Support System for Diagnosing Pulmonary Ailment through Standardized Chest X-ray Scans," *Sensors,* vol. 22, no. 19, p. 7474, 2022.

[26] A. Pathak, S. Batra and V. Sharma, "An Assessment of the Missing Data Imputation Techniques for COVID-19 Data," in *Proceedings of 3rd International Conference on Machine Learning, Advances in Computing, Renewable Energy and Communication: MARC 2021*, 2022.

[27] J. Wang and L. Perez, "The effectiveness of data augmentation in image classification using deep learning," *Convolutional Neural Networks Vis. Recognit,* vol. 11, no. 2017, pp. 1-8, 2017.

[28] D. Kermany, K. Zhang and M. Goldbaum, "Labeled optical coherence tomography (oct) and chest x-ray images for classification," *Mendeley data,* vol. 2, no. 2, p. 651, 2018.

[29] R. C. Hidayatullah and S. Violina, "Convolutional neural network architecture and data augmentation for pneumonia classification from chest X-rays images," *Int J Innov Sci Res Technol,* vol. 5, pp. 158-164, 2020.

[30] S. H. A. H. Zubair, "An efficient method to predict pneumonia from chest X-rays using deep learning approach," *The Importance Of Health Informatics In Public Health During A Pandemic,* vol. 272, p. 457, 2020.

[31] T. Mahmud, M. A. Rahman and S. A. Fattah, "CovXNet: A multi-dilation convolutional neural network for automatic COVID-19 and other pneumonia detection from chest X-ray images with transferable multi-receptive feature optimization," *Computers in biology and medicine,* vol. 122, p. 103869, 2020.

[32] V. Chouhan, S. Singh, A. Khamparia, D. Gupta, P. Tiwari, C. Moreira, R. Damaševičius and V. H. C. De Albuquerque, "A novel transfer learning based approach for pneumonia detection in chest X-ray images," *Applied Sciences,,* vol. 10, no. 2, p. 559, 2020.

[33] M. F. Hashmi, S. Katiyar, A. W. Hashmi and A. G. Keskar, "Pneumonia detection in chest X-ray images using compound scaled deep learning model," *Automatika,* vol. 62, no. 3-4, pp. 397-406, 2021.